SINGLE- AND MULTI-PLATFORM CONSTRAINED SENSOR PATH OPTIMIZATION FOR ANGLE-OF-ARRIVAL TARGET TRACKING

Kutluyıl Doğançay

School of Electrical and Information Engineering, University of South Australia
Mawson Lakes, SA 5095, Australia
phone: + (61) 883023984, fax: + (61) 883023384, email: Kutluyil.Dogancay@unisa.edu.au
web: http://people.unisa.edu.au/Kutluyil.Dogancay

ABSTRACT

This paper is concerned with optimal path planning for moving sensor platforms in angle-of-arrival (AOA) target tracking. A steering algorithm is developed to update sensor platform waypoints for a single or multiple AOA sensor platforms. The waypoint updates are derived from an iterative normalized gradient descent optimization algorithm subject to geometric and turn rate constraints. The sensor platform paths are optimized by minimizing a cost function comprising the mean-square error of predicted target position estimates produced by the extended Kalman filter and penalty functions for threat/obstacle avoidance. The effectiveness of the developed steering algorithm is illustrated with simulation examples.

1. INTRODUCTION AND BACKGROUND

Passive localization of targets from unmanned vehicles equipped with sensing devices is an important research problem that finds application in electronic warfare, surveillance and situational awareness, to name a few. A particularly important aspect of passive localization is control or steering of the moving platforms in order to maximize the localization/tracking performance among other things.

Path optimization algorithms all require a prediction of the estimation performance for a given control action. In large signal-to-noise ratio (SNR) situations the estimation performance can be approximated by the determinant of the Fisher information matrix (FIM), which is the inverse of the Cramer-Rao lower bound (CRLB). The criterion of maximizing the determinant of FIM has been extensively used in path optimization for bearings-only target motion analysis [1, 2, 3].

More recently a decentralized information-theoretic approach for unmanned aerial vehicle (UAV) path optimization for bearings-only localization was considered in [4], utilizing the information filter to facilitate distributed processing. It is shown that maximizing the mutual information gain is equivalent to maximizing the logarithm of the determinant of predicted FIM, which is in turn closely related to the *D-optimality criterion* in optimal experimental design [5].

In [6] posterior Cramer-Rao lower bound (PCRLB) is used as the optimization criterion for controlling sensor trajectories in bearings-only target tracking under the tacit assumption that the target state estimator achieves PCRLB approximately. PCRLB is a lower bound for the estimation of random parameters [7]. The proposed trajectory optimization algorithm uses a Riccati-like recursion to compute the inverse of PCRLB by means of Monte Carlo integration. It then calculates the sequence of FIMs for a range of possible sensor trajectories over a grid. The optimal sensor trajectory is determined by minimizing a measure of PCRLB, given by the maximum MSE along the x and y-axis for target location estimates.

Under the assumption that the localization estimate is nearly efficient and unbiased, UAV path optimization algorithms were developed for scan-based and hybrid (AOA/scan-based) target localization in [8, 9]. These path optimization algorithms approximate FIM by substituting the maximum likelihood target location estimate for its true value at each waypoint update.

Another research area that is closely related to UAV path planning is optimal sensor placement, which often assumes a stationary localization configuration. Optimal sensor placement configurations for AOA and time-difference-of-arrival (TDOA) sensors based on estimation uncertainty minimization (i.e., maximizing the determinant of FIM) are investigated in [10, 11].

In this paper we utilize the covariance matrix of the predicted target state estimates generated by the extended Kalman filter (EKF) to optimize mobile sensor platform trajectories. We transform the optimal steering problem into minimization of a composite cost function comprising the mean-squared error (MSE) for target state estimates and a penalty function for obstacle/threat avoidance. The control vectors for the moving platforms are calculated using a simple gradient-descent approach akin to [12, 13, 14]. The turn rate constraints are imposed by limiting the heading change for the moving platforms. The main contribution of this paper is the development of a gradient-based steering algorithm for AOA target tracking incorporating threat/obstacle avoidance and turn rate constraints.

The paper is organized as follows. Section 2 describes the target tracking problem. In Section 3 the optimal UAV path planning algorithm is developed. The implementation of geometric constraints is discussed in Section 4. Simulation studies are presented in Section 5. The paper concludes in Section 6.

2. TARGET TRACKING PROBLEM

We consider two-dimensional target tracking using AOA measurements collected by $N \geq 1$ moving platforms at discrete time instants $k = 0, 1, 2, \ldots$. The platform positions at time k are denoted by $\boldsymbol{p}_k(1), \ldots, \boldsymbol{p}_k(N)$. The target is assumed to have a nearly constant motion model [15].

The dynamical equation (the process equation) representing the motion of the target is

$$\boldsymbol{x}_{k+1} = \boldsymbol{F}\boldsymbol{x}_k + \boldsymbol{n}_k, \quad k = 0, 1, \ldots \tag{1}$$

where $\boldsymbol{x}_k = [x_k, \dot{x}_k, y_k, \dot{y}_k]^T$ is the target state vector at time k and ^{T} denotes matrix transpose. Here $[x_k, y_k]^T$ and $[\dot{x}_k, \dot{y}_k]^T$ are the target position and velocity at time k, respectively. In (1) the dynamical constraint (the state tran-

 ISSN 2076-1465

sition matrix) is given by

$$\boldsymbol{F} = \begin{bmatrix} 1 & T & 0 & 0 \\ 0 & 1 & 0 & 0 \\ 0 & 0 & 1 & T \\ 0 & 0 & 0 & 1 \end{bmatrix} \tag{2}$$

where T denotes the constant time interval between discrete-time instants k.

The process noise $\boldsymbol{n}_k$ is a zero-mean white Gaussian process with covariance matrix $\boldsymbol{Q}$, i.e., $\boldsymbol{n}_k \sim \mathcal{N}(\boldsymbol{0}, \boldsymbol{Q})$, and it accounts for unknown target maneuvers. For piecewise constant white acceleration errors, the process noise covariance matrix is [15]

$$\boldsymbol{Q} = \begin{bmatrix} q^x \boldsymbol{B} & \boldsymbol{0} \\ \boldsymbol{0} & q^y \boldsymbol{B} \end{bmatrix} \tag{3}$$

where q^x and q^y are the acceleration error variances along the x-axis and y-axis, respectively, and

$$\boldsymbol{B} = \begin{bmatrix} T^4/4 & T^3/2 \\ T^3/2 & T^2 \end{bmatrix}. \tag{4}$$

For AOA target tracking the measurement equation is

$$\boldsymbol{\theta}_k = \boldsymbol{h}(\boldsymbol{x}_k) + \boldsymbol{w}_k \tag{5}$$

where $\boldsymbol{\theta}_k$ is the vector of AOA measurements taken by N platforms at time k, $\boldsymbol{x}_k$ is the target state vector at time k and $\boldsymbol{w}_k$ is white Gaussian noise with $\boldsymbol{w}_k \sim \mathcal{N}(\boldsymbol{0}, \boldsymbol{R}_k)$. In terms of platform positions and the target position at time k we have

$$\boldsymbol{h}(\boldsymbol{x}_k) = \begin{bmatrix} \angle\big([x_k, y_k]^T - \boldsymbol{p}_k(1)\big) \\ \angle\big([x_k, y_k]^T - \boldsymbol{p}_k(2)\big) \\ \vdots \\ \angle\big([x_k, y_k]^T - \boldsymbol{p}_k(N)\big) \end{bmatrix} \tag{6}$$

where $\angle \boldsymbol{z}$ denotes the bearing angle of vector $\boldsymbol{z}$.

To account for reduced SNR for large target ranges, the AOA noise covariance is assumed to have the following range-parameterized form

$$\boldsymbol{R}_k = \sigma_b^2 \begin{bmatrix} d_k(1) & & \boldsymbol{0} \\ & \ddots & \\ \boldsymbol{0} & & d_k(N) \end{bmatrix} \tag{7a}$$

where σ_b^2 is the AOA noise variance at unit range from the target and

$$d_k(i) = \|[x_k, y_k]^T - \boldsymbol{p}_k(i)\|^\gamma. \tag{7b}$$

Here $\gamma \geq 0$ is a power loss exponent that determines the dependence of the AOA measurement noise variance on the target range. For $\gamma = 0$ we have $\boldsymbol{R}_k = \sigma_b^2 \boldsymbol{I}$, which means that the AOA noise is invariant to the target range. For nonzero γ the AOA noise variance increases with increasing target range. In the absence of compounding factors such as non-line-of-sight propagation, the AOA noise variance can be determined easily from received signal power and sensor characteristics.

In this paper we employ the EKF to estimate the target state vector. It is possible to extend the discussion to other recursive estimators such as the unscented Kalman filter. The prediction and update equations of the EKF are given by

State Prediction:

$$\boldsymbol{x}_{k|k-1} = \boldsymbol{F}\boldsymbol{x}_{k-1|k-1} \tag{8a}$$

$$\boldsymbol{P}_{k|k-1} = \boldsymbol{F}\boldsymbol{P}_{k-1|k-1}\boldsymbol{F}^T + \boldsymbol{Q} \tag{8b}$$

State Update:

$$\boldsymbol{x}_{k|k} = \boldsymbol{x}_{k|k-1} + \boldsymbol{K}_k \tilde{\boldsymbol{\theta}}_k \tag{8c}$$

$$\boldsymbol{P}_{k|k} = (\boldsymbol{I} - \boldsymbol{K}_k \boldsymbol{H}_k)\boldsymbol{P}_{k|k-1} \tag{8d}$$

$$\tilde{\boldsymbol{\theta}}_k = \boldsymbol{\theta}_k - \boldsymbol{h}(\boldsymbol{x}_{k|k-1}) \tag{8e}$$

$$\boldsymbol{K}_k = \boldsymbol{P}_{k|k-1}\boldsymbol{H}_k^T(\boldsymbol{H}_k \boldsymbol{P}_{k|k-1}\boldsymbol{H}_k^T + \boldsymbol{R}_k)^{-1} \tag{8f}$$

where $\boldsymbol{x}_{k|k-1}$ is the state prediction at time k given all measurements up to time $k-1$, $\boldsymbol{x}_{k|k}$ is the filtered state estimate at time k, $\tilde{\boldsymbol{\theta}}_k$ is the innovations vector at time k, and $\boldsymbol{P}_{k|k}$ is the error covariance matrix for the filtered state estimate at time k. In the event the matrix inversion in (8f) does not exist due to rank deficiency it can be replaced by pseudo-inverse. The $N \times 4$ matrix $\boldsymbol{H}_k$ is the Jacobian of the nonlinear measurement function $\boldsymbol{h}(\boldsymbol{x}_k)$ evaluated at $\boldsymbol{x}_{k|k-1}$:

$$\boldsymbol{H}_k = \begin{bmatrix} -\frac{d^y_{k|k-1}(1)}{\|\boldsymbol{d}_{k|k-1}(1)\|^2} & 0 & \frac{d^x_{k|k-1}(1)}{\|\boldsymbol{d}_{k|k-1}(1)\|^2} & 0 \\ -\frac{d^y_{k|k-1}(2)}{\|\boldsymbol{d}_{k|k-1}(2)\|^2} & 0 & \frac{d^x_{k|k-1}(2)}{\|\boldsymbol{d}_{k|k-1}(2)\|^2} & 0 \\ \vdots & \vdots & \vdots & \vdots \\ -\frac{d^y_{k|k-1}(N)}{\|\boldsymbol{d}_{k|k-1}(N)\|^2} & 0 & \frac{d^x_{k|k-1}(N)}{\|\boldsymbol{d}_{k|k-1}(N)\|^2} & 0 \end{bmatrix} \tag{9}$$

where

$$\boldsymbol{d}_{k|k-1}(i) = \begin{bmatrix} d^x_{k|k-1}(i) \\ d^y_{k|k-1}(i) \end{bmatrix} = \begin{bmatrix} x_{k|k-1} \\ y_{k|k-1} \end{bmatrix} - \boldsymbol{p}_k(i), \quad i = 1, \ldots, N \tag{10}$$

and

$$\boldsymbol{x}_{k|k-1} = [x_{k|k-1}, \dot{x}_{k|k-1}, y_{k|k-1}, \dot{y}_{k|k-1}]^T. \tag{11}$$

The EKF recursions are initialized by

$$\boldsymbol{x}_{0|-1} = E\{\boldsymbol{x}_0\} \quad \text{and} \quad \boldsymbol{P}_{0|-1} = \mathrm{Cov}\{\boldsymbol{x}_0\}. \tag{12}$$

3. PATH OPTIMIZATION

The objective of sensor path optimization is to determine moving platform trajectories so as to maximize the tracking performance in the presence of path constraints such as turn rates and any threat/collision avoidance.

The waypoints at time instant $k+1$ are given by

$$\boldsymbol{p}_{k+1}(i) = \boldsymbol{p}_k(i) + \boldsymbol{u}_k(i), \quad i = 1, \ldots, N, \quad k = 0, 1, \ldots \tag{13}$$

where $\boldsymbol{p}_k(i)$ is the 2D position vector of the ith UAV in Cartesian coordinates at waypoint update k and $\boldsymbol{u}_k(i)$ is the control input for the ith platform with norm and turn rate constraints

$$\|\boldsymbol{u}_k(i)\| = v_k(i)T, \quad |\angle \boldsymbol{u}_{k+1}(i) - \angle \boldsymbol{u}_k(i)| \leq \varphi. \tag{14}$$

Here $v_k(i)$ is the cruising speed of the ith platform at time k and φ is the maximum turn rate in radians. The control vector norm $\|\boldsymbol{u}_k(i)\|$ is assumed to be constant, which implies that $v_k(i)$ is time-invariant.

Optimal path planning requires the selection of control inputs in order to minimize a cost function that measures optimality. In our case the cost function to be minimized is the MSE of *predicted* state estimates, which is approximately given by

$$J(\boldsymbol{\pi}_k) = \boldsymbol{P}_{k+1|k}(1,1) + \boldsymbol{P}_{k+1|k}(3,3), \quad \boldsymbol{\pi}_k = \begin{bmatrix} \boldsymbol{p}_k(1) \\ \vdots \\ \boldsymbol{p}_k(N) \end{bmatrix} \tag{15}$$

where $\boldsymbol{P}_{k+1|k}(i,j)$ denotes the (i,j)th entry of $\boldsymbol{P}_{k+1|k}$. The cost function $J(\boldsymbol{\pi}_k)$ is approximate since $\boldsymbol{P}_{k+1|k}$ is not the true covariance of state prediction as a result of approximate linearization used by the EKF. The path optimization problem can be solved by gradient-descent waypoint updates:

$$\boldsymbol{p}_{k+1}(i) = \boldsymbol{p}_k(i) - \mu_k(i)\frac{\partial J(\boldsymbol{\pi}_k)}{\partial \boldsymbol{p}_k(i)}, \quad i = 1,\ldots,N, \quad k = 0,1,\ldots \tag{16}$$

where $\mu_k(i)$ is a time-varying step-size that normalizes control inputs in order to satisfy the norm constraint in (14):

$$\mu_k(i) = \frac{v_k(i)T}{\|\partial J(\boldsymbol{\pi}_k)/\partial \boldsymbol{p}_k(i)\|}. \tag{17}$$

The waypoint update equation (16) can be equivalently written as

$$\boldsymbol{\pi}_{k+1} = \boldsymbol{\pi}_k - \boldsymbol{M}_k\frac{\partial J(\boldsymbol{\pi}_k)}{\partial \boldsymbol{\pi}_k}, \quad k = 0,1,\ldots$$
$$\boldsymbol{M}_k = \begin{bmatrix} \mu_k(1)\boldsymbol{I}_2 & & \boldsymbol{0} \\ & \ddots & \\ \boldsymbol{0} & & \mu_k(N)\boldsymbol{I}_2 \end{bmatrix}. \tag{18}$$

Here $\boldsymbol{I}_2$ denotes the 2×2 identity matrix.

Even though it is possible to obtain algebraic expressions for the gradient of $J(\boldsymbol{\pi}_k)$, we opt for numerical computation using a first-order finite difference approximation. This provides us with flexibility for cost function modifications, e.g., to cater for soft constraints. Let

$$\frac{\partial J(\boldsymbol{\pi}_k)}{\partial \boldsymbol{\pi}_k} = [\alpha_k(1), \alpha_k(2), \cdots, \alpha_k(2N)]^T. \tag{19}$$

Then the first-order finite difference approximation for the gradient vector is

$$\alpha_k(i) \approx \frac{J(\boldsymbol{\pi}_k + \boldsymbol{\delta}_i) - J(\boldsymbol{\pi}_k)}{\delta} \tag{20}$$

where $\boldsymbol{\delta}_i$ is a $2N\times 1$ column vector with zero entries except for the ith entry which is equal to a small positive real number δ:

$$\boldsymbol{\delta}_i = \big[0,\ \cdots,\ 0,\ \underbrace{\delta}_{i\text{th entry}},\ 0,\ \cdots,\ 0\big]^T. \tag{21}$$

In (20) division by δ can be absorbed into normalization of control inputs. Thus the gradient based steering algorithm in (18) can be replaced with

$$\boldsymbol{\pi}_{k+1} = \boldsymbol{\pi}_k - \boldsymbol{N}_k \begin{bmatrix} J(\boldsymbol{\pi}_k + \boldsymbol{\delta}_1) - J(\boldsymbol{\pi}_k) \\ \vdots \\ J(\boldsymbol{\pi}_k + \boldsymbol{\delta}_{2N}) - J(\boldsymbol{\pi}_k) \end{bmatrix}, \quad k = 0,1,\ldots \tag{22}$$

where $\boldsymbol{N}_k$ is a $2N\times 2N$ diagonal normalization matrix

$$\boldsymbol{N}_k = \begin{bmatrix} \eta_k(1)\boldsymbol{I}_2 & & \boldsymbol{0} \\ & \ddots & \\ \boldsymbol{0} & & \eta_k(N)\boldsymbol{I}_2 \end{bmatrix} \tag{23}$$

and

$$\eta_k(i) = \frac{v_k(i)T}{\left\| \begin{bmatrix} J(\boldsymbol{\pi}_k + \boldsymbol{\delta}_{2i-1}) - J(\boldsymbol{\pi}_k) \\ J(\boldsymbol{\pi}_k + \boldsymbol{\delta}_{2i}) - J(\boldsymbol{\pi}_k) \end{bmatrix} \right\|}. \tag{24}$$

When calculating the approximate gradients, the only quantities that are affected by the perturbation of $\boldsymbol{\pi}_k$ are the measurement noise covariance matrix $\boldsymbol{R}_k$ and the Jacobian matrix $\boldsymbol{H}_k$. Consequently the calculation of $J(\boldsymbol{\pi}_k + \boldsymbol{\delta}_i)$ only involves re-calculation of $\boldsymbol{H}_k$ and $\boldsymbol{K}_k$ in the EKF equation (8d).

4. PATH CONSTRAINTS

4.1 Hard Constraints

It is often imperative that a certain minimum clearance between the moving platforms and the target be maintained in order to ensure that (i) the platforms are not detected by the target and (ii) signal reception from the target is not interrupted.

A simple way to implement distance restrictions is to impose a circular hard constraint around the target location. The hard constraint is activated whenever a waypoint update results in a platform crossing the circular boundary:

- If $\|\boldsymbol{p}_{k+1}(i) - [x_{k+1|k}, y_{k+1|k}]^T\| > d_{\min}$,

$$\boldsymbol{p}_{k+1}(i) = \boldsymbol{p}_k(i) + \boldsymbol{u}_k(i) \tag{25}$$

- Otherwise, rotate $\boldsymbol{u}_k(i)$ by a minimum angle so that $\boldsymbol{p}_{k+1}(i)$ is on the boundary of the hard constraint, i.e., $\|\boldsymbol{p}_{k+1}(i) - [x_{k+1|k}, y_{k+1|k}]^T\| = d_{\min}$.

Here $d_{\min}$ is the minimum clearance from the target (i.e., the radius of the hard constraint), $[x_{k+1|k}, y_{k+1|k}]^T$ is the prediction of the target location produced by the EKF, and $\boldsymbol{u}_k(i)$ is the control input for the ith platform.

4.2 Soft Constraints

Suppose that there are K threats at known locations $\boldsymbol{c}(i)$, $i = 1,\ldots,K$, to be avoided by the moving sensor platforms. Soft constraints can be created around threat locations to steer the platforms away from them. To do this we need to modify $J(\boldsymbol{\pi}_k)$ so that it tends to infinity at the $\boldsymbol{c}(i)$. This is easily achieved by introducing maxima at the $\boldsymbol{c}(i)$:

$$J_c(\boldsymbol{\pi}_k) = J(\boldsymbol{\pi}_k) + \sum_{i=1}^{K}\sum_{j=1}^{N}\frac{1}{1-\exp\{-\frac{1}{\kappa_i}\|\boldsymbol{p}_k(j) - \boldsymbol{c}(i)\|^2\}}. \tag{26}$$

Here $\kappa_i > 0$, $i = 1,\ldots,K$, is the risk parameter for the ith threat; i.e., the larger κ_i the larger the clearance.

4.3 Turn-Rate Constraints

Turn rate constraints have priority over other constraints and therefore they are applied last. If, for a given control vector, the constraint $|\angle\boldsymbol{u}_{k+1}(i) - \angle\boldsymbol{u}_k(i)| \le \varphi$ is not met, then the heading direction of the control vector is adjusted so that $|\angle\boldsymbol{u}_{k+1}(i) - \angle\boldsymbol{u}_k(i)| = \varphi$. Significant conflicts between turn rate and hard constraints can be resolved simply by setting $d_{\min}$ to a larger value than what is desired.

5. SIMULATION STUDIES

The first two simulation examples consider stationary target localization by a team of moving sensor platforms. For a stationary target the process equation (1) becomes

$$\boldsymbol{x}_{k+1} = \boldsymbol{F}\boldsymbol{x}_k, \quad k = 0,1,\ldots \tag{27}$$

where $\boldsymbol{x}_0 = [x_0, 0, y_0, 0]^T$, i.e., $\dot{x}_k = 0$, $\dot{y}_k = 0$ and $\boldsymbol{n}_k = \boldsymbol{0}$.

The stationary target coordinates are $[5,1]^T$ km. A team of three sensor platforms with $v_k(i) = 30$ m/s, $i = 1,2,3$, and $\varphi = 40^\circ$ are used to geolocate the target. The parameters for the steering algorithm are $T = 2$ s, $\delta = 1$ m and $d_{\min} = 0.5$ km. The initial UAV positions at $k = 0$ are $\boldsymbol{p}_0(1) = [1,2]^T$ km, $\boldsymbol{p}_0(2) = [0.5,0]^T$ km and $\boldsymbol{p}_0(3) = [1,-2]^T$ km. The localization geometry is known to have a threat at $\boldsymbol{c}_1 = [3,-1.5]^T$ km to be avoided by a soft constraint with risk parameter $\kappa_1 = 0.08$. The AOA noise standard deviation at unit range is $\sigma_b = 1^\circ$ and the power loss exponent is $\gamma = 0.2$ (the target range is converted to meters

when calculating the AOA covariance matrix). The EKF assumes zero acceleration error variances, i.e., $q^x = q^y = 0$, and is initialized to $\boldsymbol{x}_{0|-1} = [3, 0, 0, 0]^T$ and $\boldsymbol{P}_{0|-1} = 5\boldsymbol{I}$.

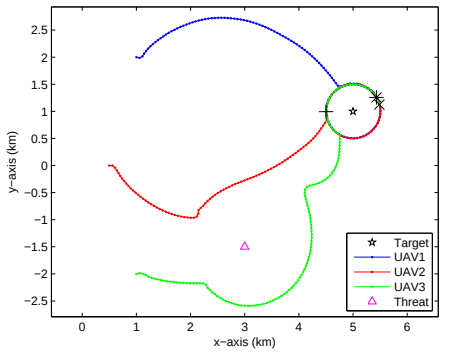

(a)

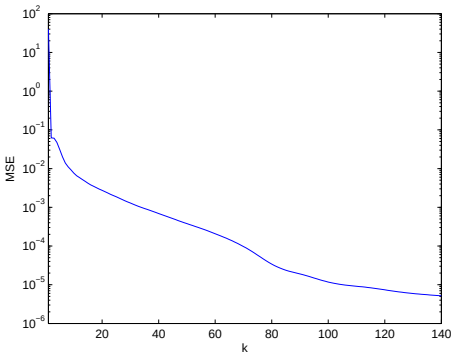

(b)

Figure 1: (a) Optimal sensor paths for geolocating a stationary target subject to a soft constraint, (b) evolution of MSE. The final sensor locations are marked with $*$, $+$ and $\times$ in (a).

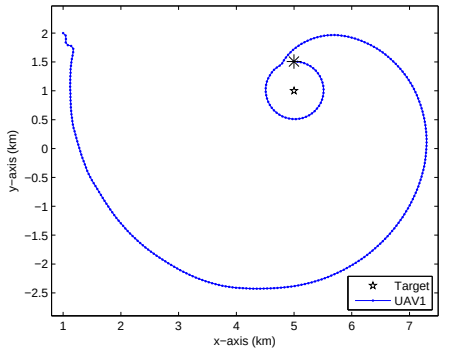

Figure 2: Optimal localization trajectory for a single platform with AOA sensor.

Fig. 1 shows the optimal sensor paths generated by (22) using $J_c(\boldsymbol{\pi}_k)$, along with the evolution of MSE. The soft constraint keeps the sensor platforms away from the threat location $\boldsymbol{c}_1$. The hard constraint around the target restricts the movement of the sensor platforms by rotating the control vectors onto the circular boundary.

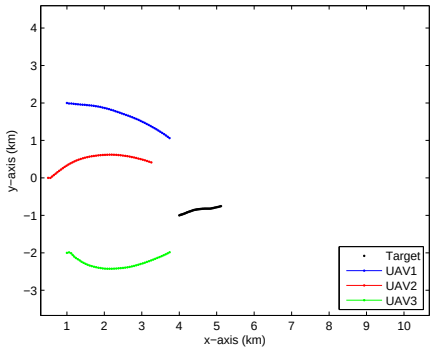

(a)

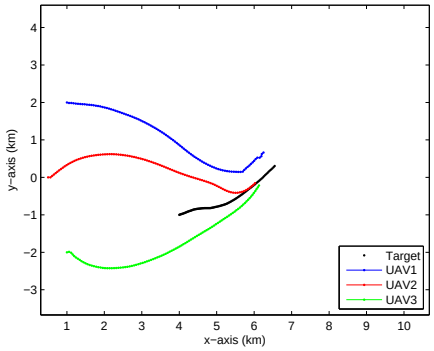

(b)

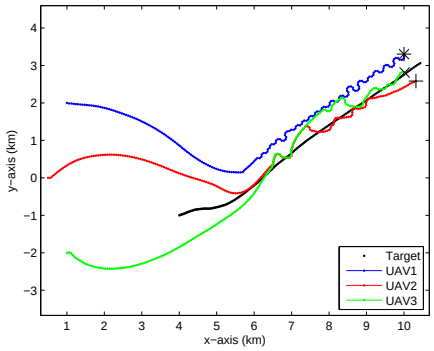

(c)

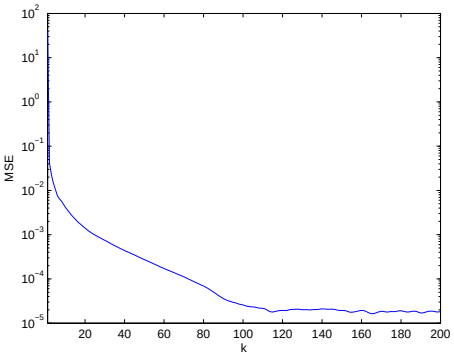

(d)

Figure 3: Optimal sensor platform paths for target tracking after (a) 50 waypoint updates, (b) 100 waypoint updates, and (c) 200 waypoint updates; (d) evolution of MSE. The final sensor locations are marked with large $*$, $+$ and $\times$ in (c).

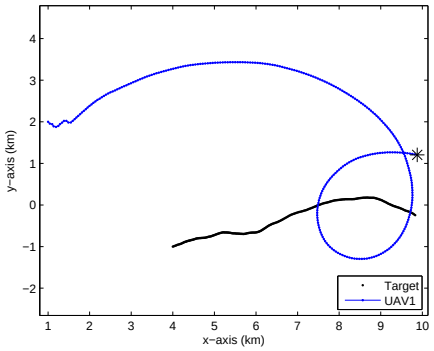

Figure 4: Optimal target tracking trajectory for a single platform.

Intuitively the optimal trajectory for a single sensor platform would be a spiral flight path around the stationary target with the distance between the sensor and the target getting gradually smaller. The next simulation example will demonstrate this. We have a single sensor platform starting at $\boldsymbol{p}_0(1) = [1, 2]^T$ km. Fig. 2 shows the simulated trajectory. A circular trajectory around the target would yield the optimal AOA localization performance. If, however, the range is not restricted, the optimal trajectory becomes a spiral path combining circular movement with an incremental range reduction.

The next two simulations consider target tracking. The target has a nearly constant velocity motion model with initial target state $\boldsymbol{x}_0 = [4, 0.01, -1, 0.004]^T$ and acceleration error variances $q^x = 2 \times 10^{-8}$ and $q^y = -10^{-7}$. The EKF assumes $q^x = q^y = 10^{-9}$. Fig. 3 shows the simulated optimal sensor platform paths and the evolution of MSE. Several observations are in order. The sensor platforms forgo baseline expansion for getting closer to the target since the target is moving away from the platforms and the target range needs to reduced to achieve better tracking performance. The turn rate constraints and constant platform speeds produce some loop maneuvers on hard constraint boundaries, which is seen in Fig. 3(c).

Fig. 4 shows a simulated optimal sensor trajectory for a single AOA platform. In this case the optimal trajectory is not unique as it is influenced by the target maneuvers. The observability of the target is improved by steering the sensor platform so that it outmaneuvers the target. Once the platform overtakes the target the path optimization algorithm steers it in a circular path around the target to achieve this.

6. CONCLUSION

We have developed a sensor steering algorithm for AOA target tracking based on the minimization of the target state estimation errors subject to path constraints. For illustration purposes the target is assumed to have a nearly constant velocity motion model. The target state (position and velocity) is recursively estimated by the EKF. The platform waypoints are computed at discrete time intervals by minimizing the MSE of predicted target state estimates produced by the EKF, as well as, any soft constraint cost function, leading to an iterative waypoint update algorithm that can be implemented in real time. The paper also proposes a rotation-based method for implementing a geometric hard constraint around the target and applies turn rate constraints by limiting changes in platform headings. The developed steering algorithm is shown to perform well both in localization of a stationary target and tracking of a moving target with unknown dynamics.

REFERENCES

[1] J. P. Le Cadre and C. Jauffret, "Discrete-time observability and estimability analysis for bearings-only target motion analysis," *IEEE Trans. Aerospace and Electronic Systems*, vol. 33, no. 1, pp. 178–201, January 1997.

[2] J. M. Passerieux and D. Van Cappel, "Optimal observer maneuver for bearings-only tracking," *IEEE Trans. on Aerospace and Electronic Systems*, vol. 34, no. 3, pp. 777–788, July 1998.

[3] Y. Oshman and P. Davidson, "Optimization of observer trajectories for bearings-only target localization," *IEEE Trans. on Aerospace and Electronic Systems*, vol. 35, no. 3, pp. 892–902, 1999.

[4] B. Grocholsky, A. Makarenko, and H. Durrant-Whyte, "Information-theoretic coordinated control of multiple sensor platforms," in *Proc. of IEEE Int. Conference on Robotics and Automation, ICRA '03*, vol. 1, Taipei, Taiwan, September 2003, pp. 1521–1526.

[5] D. Uciński, *Optimal Measurement Methods for Distributed Parameter System Identification*. Boca Radon, Florida: CRC Press, 2005.

[6] M. L. Hernandez, "Optimal sensor trajectories in bearings-only tracking," in *Proc. of 7th Int. Conf. on Information Fusion, FUSION 2004*, vol. 2, Stockholm, Sweden, June 2004, pp. 893–900.

[7] H. L. Van Trees, *Detection, Estimation, and Modulation Theory, Part I*. New York: Wiley, 1968.

[8] K. Doğançay, "Online optimization of receiver trajectories for scan-based emitter localization," *IEEE Trans. on Aerospace and Electronic Systems*, vol. 43, no. 3, pp. 1117–1125, July 2007.

[9] ——, "Optimized path planning for UAVs with AOA/scan based sensors," in *Proc. of 15th European Signal Processing Conference, EUSIPCO 2007*, Poznan, Poland, September 2007.

[10] K. Doğançay and H. Hmam, "Optimal angular sensor separation for AOA localization," *Signal Processing*, vol. 88, no. 5, pp. 1248–1260, May 2008.

[11] ——, "On optimal sensor placement for time-difference-of-arrival localization utilizing uncertainty minimization," in *Proc. of European Signal Processing Conference, EUSIPCO 2009*, Glasgow, UK, August 2009, pp. 1136–1140.

[12] J. R. Spletzer and C. J. Taylor, "Dynamic sensor planning and control for optimally tracking targets," *Int. Journal of Robotics Research*, vol. 22, no. 1, pp. 7–20, January 2003.

[13] T. H. Chung, J. W. Burdick, and R. M. Murray, "A decentralized motion coordination strategy for dynamic target tracking," in *Proc. 2006 IEEE Int. Conf. Robotics and Automation*, Florida, May 2006, pp. 2416–2422.

[14] P. Yang, R. A. Freeman, and K. M. Lynch, "Distributed cooperative active sensing using consensus filters," in *Proc. 2007 IEEE Int. Conf. Robotics and Automation*, Roma, Italy, April 2007, pp. 405–410.

[15] Y. Bar-Shalom and W. D. Blair, Eds., *Multitarget-Multisensor Tracking: Applications and Advances*. Boston, MA: Artech House, 2000, vol. III.